Check for updates

Received: 14 August 2023 | Revised: 2 February 2024 | Accepted: 17 March 2024

DOI: 10.1002/cbin.12161

RESEARCH ARTICLE

Cell Biology International WILEY

# BMP7-induced osteoblast differentiation requires hedgehog signaling and involves nuclear mechanisms of gene expression control

Georgia da Silva Feltran[1] | Amanda Fantini de Andrade[1] | Célio Jr da C. Fernandes[1] | Rodrigo A. Foganholi da Silva[1,2,3] | Willian F. Zambuzzi[1]

[1]Lab. of Bioassays and Cellular Dynamics, Department of Chemical and Biological Sciences, Institute of Biosciences, UNESP: São Paulo State University, Botucatu, São Paulo, Brazil

[2]Department of Biology, Dental School, University of Taubaté, Taubaté, São Paulo, Brazil

[3]CEEpiRG—Center for Epigenetic Study and Genic Regulation, Program in Environmental and Experimental Pathology, Paulista University, São Paulo, São Paulo, Brazil

**Correspondence**
Willian F. Zambuzzi, Laboratório de Bioensaios e Dinâmica Celular, Depto de Ciências Químicas e Biológicas, Instituto de Biociências—IBB—UNESP, São Paulo, Brazil.
Email: w.zambuzzi@unesp.br

**Funding information**
Fundação de Amparo à Pesquisa do Estado de São Paulo, Grant/Award Numbers: 2014/22689-3, 2016/01139-0, 2019/26854-2; Conselho Nacional de Desenvolvimento Científico e Tecnológico, Grant/Award Numbers: 301498/2022-9, 314166/2021-1

## Abstract

During the morphological changes occurring in osteoblast differentiation, Sonic hedgehog (Shh) plays a crucial role. While some progress has been made in understanding this process, the epigenetic mechanisms governing the expression of Hh signaling members in response to bone morphogenetic protein 7 (BMP7) signaling in osteoblasts remain poorly understood. To delve deeper into this issue, we treated pre-osteoblasts (pObs) with 100 ng/mL of BMP7 for up to 21 days. Initially, we validated the osteogenic phenotype by confirming elevated expression of well-defined gene biomarkers, including *Runx2*, *Osterix*, Alkaline Phosphatase (*Alp*), and bone sialoprotein (Bsp). Simultaneously, Hh signaling-related members Sonic (Shh), Indian (Ihh), and Desert (Dhh) Hedgehog (Hh) exhibited nuanced modulation over the 21 days in vitro period. Subsequently, we evaluated epigenetic markers, and our data revealed a notable change in the CpG methylation profile, considering the methylation/hydroxymethylation ratio. CpG methylation is a reversible process regulated by DNA methyltransferases and demethylases, including Ten-eleven translocation (Tets), which also exhibited changes during the acquisition of the osteogenic phenotype. Specifically, we measured the methylation pattern of Shh-related genes and demonstrated a positive Pearson correlation for GLI Family Zinc Finger 1 (Gli1) and Patched (Ptch1). This data underscores the significance of the epigenetic machinery in modulating the BMP7-induced osteogenic phenotype by influencing the activity of Shh-related genes. In conclusion, this study highlights the positive impact of epigenetic control on the expression of genes related to hedgehog signaling during the morphogenetic changes induced by BMP7 signaling in osteoblasts.

KEYWORDS
BMP, bone, bone healing, epigenetic, hedgehog, osteoblast differentiation

**Abbreviations:** 5-hmeC, 5-hydroxymethylcytidine; 5-meC, 5-methylcytosine; Actb, β-actin; Alp, ALP, alkaline phosphatase; BMP7, bone morphogenetic protein 7; BMPs, morphogenetic proteins; BSP, bone sialoprotein; Cyclo, cyclopamine; Dhh, desert hedgehog; Dnmt1, DNA (cytosine-5)-methyltransferase 1; Dnmt3A, DNA (cytosine-5)-methyltransferase 3A; Dnmt3B, DNA (cytosine-5)-methyltransferase 3B; DNMTs, DNA methyltransferases; FBS, fetal bovine serum; GANT-61, Gli1 antagonist.; Gapdh, glyceraldehyde-3-phosphate dehydrogenase; gDNA, genomic DNA; Gli1, GLI Family Zinc Finger 1; Gli2, GLI Family Zinc Finger 2; Gli3, GLI Family Zinc Finger 3; Hg, hedgehog; Hh, Sonic hedgehog; Ihh, Indian hedgehog; ng/mL, nanagrams per milliliter; Otx, transcription factor Sp7; pObs, pre-osteoblasts; Ptch1, Patched homolog 1; rhBMP-7, recombinant human BMP-7; Runx2, runt-related transcription factor-2; Shh, SHH, Sonic hedgehog; Sufu, Suppressor of fused homolog; T4-BGT, T4-β-glucosyltransferase; Tet1, Ten-eleven translocation methylcytosine dioxygenase 1; Tet2, Ten-eleven translocation methylcytosine dioxygenase 2; Tet3, Ten-eleven translocation methylcytosine dioxygenase 3; Tets, Ten-eleven translocation.

Georgia da Silva Feltran and Amanda Fantini de Andrade contributed equally to this study.

 © 2024 International Federation for Cell Biology. 

## 1 | INTRODUCTION

Bone healing progresses through a sequential and well-defined series of biological events involving the activation of extracellular signaling molecules that initiate intracellular pathways during the osteogenic phenotype (Marumoto et al., 2017). Among these active molecules, morphogenetic proteins like bone morphogenetic proteins (BMPs) and members of the Sonic (Sh), Indian (Ih), and Desert (Dh) hedgehog (Hh) family merit closer examination in the context of bone regeneration. The objective of this analysis is to enhance our comprehension of osteogenesis and its subsequent impact on bone remodeling. During endochondral ossification, Sonic hedgehog (Shh) collaborates synergistically with the BMP pathway. Some studies also indicate that Shh increases the commitment of mesenchymal lineages and calvaria cells to the osteoblastic lineage upon activation of the BMP pathway (Bae et al., 2016; James et al., 2010; Spinella-Jaegle et al., 2001).

While BMP signaling has been extensively explored in bone studies (Carreira et al., 2015), the involvement of Hh signaling during osteoblast differentiation remains unclear. However, evidence suggests that specific Sonic hedgehog (Shh) plays a pivotal role in orchestrating the morphological changes of osteoblasts, driving the transition to osteocytes (Marumoto et al., 2017). Furthermore, the maintenance of activated Hh signaling in mature osteoblasts is linked to the development of fragile long bones with significantly reduced bone density due to increased osteoclast activity (Kiuru et al., 2009; Mak et al., 2008; Tian et al., 2012). This phenomenon can be attributed to osteocytes being recognized as the primary source of RANKL in vertebrates. From a mechanistic standpoint, members of the hedgehog (Hh) family interact with Patched (Ptch1) along the plasma membrane, facilitating the recruitment of Gli1, which is then translocated to the nucleus (Caradu et al., 2018; Lopez-Rios, 2016; da Silva Feltran et al., 2019). Generally, Gli transcription factors mediate all Hh signaling in mammals, with GLI Family Zinc Finger 2 (Gli2) and GLI Family Zinc Finger 3 (Gli3) serving as the primary contributors, while Gli1 amplifies the signal response (Bai et al., 2002). Taking this into account, we can affirm that Hh signaling is a key morphogenetic factor in regulating bone development, homeostasis and repair and its modulation by epigenetic regulation is hypothesized here.

Epigenetic mechanism (especially DNA methylation) has gained relevance in studies addressing the molecular basis of bone biology (Eslaminejad et al., 2013; Vrtačnik et al., 2014). Concerning bone homeostasis, earlier research indicates that the epigenetic machinery governs the transcription of key genes associated with osteogenic differentiation (Assis et al., 2021; Ferreira et al., 2022; da Silva et al., 2020; da Silva, Fuhler, et al., 2019; Vrtačnik et al., 2014). On a global scale, epigenetic mechanisms encompass acetylation, methylation, micro-RNA, and long non-coding RNA, intricately orchestrating the transcription of specific genes (Ergun & Oztuzcu, 2015; Lappalainen & Greally, 2017; Li et al., 2018; Lorenzen & Thum, 2016). In the context of bone tissue, it is well-established that DNA methylation plays an undeniable regulatory role during osteoblast differentiation. The accumulation of molecular errors over time can lead to the disruption of normal epigenetic patterns, contributing to skeletal disorders (Marini et al., 2016).

In a physiological context, osteoblasts exhibit constitutive responsiveness to BMPs, inducing a differentiated phenotype by modifying the gene repertoire, which includes members associated with hedgehog (Hh) signaling. This study represents one of the early explorations into the role of DNA methylation in regulating gene expression of Hh-related members during the stages of osteoblast differentiation. Previous studies have indicated that DNA hypermethylation negatively influences the BMP/SHH pathway in other tissues (Liu et al., 2021; Wang et al., 2017; Zhou et al., 2023). Our findings suggest a synergistic relationship between the BMP and Hh signaling pathways, with this interplay appearing to coordinate the osteogenic phenotype of bone cells, dynamically influenced by epigenetic mechanisms.

## 2 | METHODS

### 2.1 | Reagents and antibodies

Dexamethasone (D2915), ascorbic acid (A5960), β-glycerolphosphate (G9422), Phenol/chloroform (p3803), cyclopamine hydrate (C4116), and G8923 (G8923) were purchased from Sigma Chemical Co. Gotaq qPCR master mix (A6002) was purchased from PROMEGA (Madison). DNase I (18068015), High-Capacity cDNA Reverse Transcription and TRIzol (15596018) were purchased from Life Technologies/Molecular Probes, Inc. Oligonucleotides (primers) were purchased from Exxtend Biotechnology. T4-β-glucosyltransferase (T4-BGT) MspI and HpaII restriction enzymes were obtained from New England Biolabs. All the other chemicals and reagents used in this study were of analytical grade purchased from commercial sources.

### 2.2 | Cell culture

Pre-osteoblasts, MC3T3-E1 Subclone 4 (ATCC CRL-2593), was cultured in αMEM medium containing antibiotics (100 U/mL penicillin, 100 mg/mL streptomycin), ribonucleosides and deoxyribonucleosides, supplemented with 10% fetal bovine serum (FBS) (Nutricell) and maintained at 37°C in a humidified atmosphere containing 5% $CO_2$. To differentiate the osteoblasts, pre-osteoblasts (pObs) were seeded into 6-well plates ($25 \times 10^4$ cells) in αMEM supplemented with 10% FBS. After 24 h of incubation, the medium was replaced by using a osteogenic medium, containing 100 ng/mL recombinant human BMP-7 (rhBMP-7) up to 7, 14, and 21 days. The control group was maintained using classical αMEM supplemented with 10% FBS, ribonucleosides, and deoxyribonucleosides.

### 2.3 | RNA isolation and complementary DNA (cDNA) synthesis

Respecting the timeline of the samples harvesting, the total RNA was extracted using Ambion TRIzol Reagent (Life Sciences—Fisher

10958355, 2024, 7, Downloaded from https://onlinelibrary.wiley.com/doi/10.1002/cbin.12161 by UNIP - Universidade Paulista, Wiley Online Library on [04/07/2025]. See the Terms and Conditions (https://onlinelibrary.wiley.com/terms-and-conditions) on Wiley Online Library for rules of use; OA articles are governed by the applicable Creative Commons License

Scientific Inc.) and its concentration and purity of total RNA determined measuring the absorbance at 260/280 nm (NANODROP 2000, Thermo) (Rio et al., 2010). After treatment of total RNA with DNase I (Invitrogen), the cDNA was synthesized from 2 µg total RNA with High-Capacity cDNA Reverse Transcription Kit (Applied Biosystems) in a standard 20 µL volume according to the protocol.

## 2.4 | Gene expression

Osteogenic differentiation markers [runt-related transcription factor-2 (Runx2), transcription factor Sp7 (Osterix), and alkaline phosphatase (Alp)] were evaluated. Shh-pathway members [Sonic hedgehog (Shh), protein Patched homolog 1 (Ptch1), Suppressor of fused homolog (Sufu), glioma-associated oncogene family zinc finger 1 (Gli1)] and DNA methylation control-related genes [DNA (cytosine-5)-methyltransferase 1 (Dnmt1), DNA (cytosine-5)-methyltransferase 3A (Dnmt3A), DNA (cytosine-5)-methyltransferase 3B (Dnmt3B), Ten-eleven translocation methylcytosine dioxygenase 1 (Tet1), Ten-eleven translocation methylcytosine dioxygenase 2 (Tet2), and Ten-eleven translocation methylcytosine dioxygenase 3 (Tet3)] gene expression in osteoblastic cells was quantified using SYBR green quantitative PCR analysis. Real-time PCR amplification was performed with the QuantStudio® 3 Real-Time PCR (Thermo Fisher Scientific). The 10 µL PCR system consisted of 1 µL cDNA (50 ng), 0.5 µmol forward primer, 0.5 µmol reverse primer, 5 µL SYBR green qPCR mix and 3 µL ultrapure DEPC-treated Water. PCR primers were designed using Primer3 Input (version 0.4.0) software (Untergasser et al., 2012). The secondary structures and annealing temperatures analysis by Beacon Designer program, Free Edition (http://www.premierbiosoft.com/) and confirmed by the in silico PCR (https://genome.ucsc.edu/). Primer 5.0 software and primers synthesis were acquired from Invitrogen Co. (Life Technologies). Primers sequences and CR conditions are presented in Table 1. Gene expression was expressed as compared to control cells by $^{\Delta\Delta}$CT method, using average CT values of β-actin (*Actb*) and glyceraldehyde-3-phosphate dehydrogenase (*Gapdh*) represented on the plate as housekeeping controls in three independent experiments in duplicate. To establish a loading control, *Actb* and *Gapdh* were used as reference genes. The $^{\Delta\Delta}$CT method was used to calculate expression values.

## 2.5 | DNA extraction and gene promoter methylation analysis

The gene promoter methylation analysis was performed after genomic DNA (gDNA) extraction with phenol/chloroform protocol and further treated with T4-β-glucosyltransferase (T4-BGT) (New England Biolabs). This enzyme adds glucose moiety to 5-hydroxymethylcytidin (5-hmeC) (gDNA) to distinguish amongst DNA methylation and hydroxymethylation (da Silva, Fernandes, et al., 2019). For this, each sample was distributed on three tubes containing the same concentration of gDNA (400 ng) that were treated with 40 mM UDP glucose and T4-BGT (1 unit) for 1 h at 37°C and inactivated by 10 min at 65°C. Next, were digested with *Msp*I, *Hpa*II and $H_2O$ for 1 h at 37°C according to the manufacturer's instructions (New England BioLabs). For the gene specific methylation analyze, the reactions were carried out in a total of 10 µL, containing PowerUp™ SYBR™ Green Master Mix 2x (5 µL) (Applied Biosystems), 0.5 µM of each primer, 20 ng of gDNA and nuclease free $H_2O$ a QuantStudio® 3 Real-Time PCR (Thermo Fisher Scientific). All the primers set were designed on gene regulatory regions content DNaseI hypersensitivity clusters sites, histone modifications marks, CpG regions and transcription factors binding sites, with Primer3 Input (version 0.4.0) software. The secondary structures and annealing temperatures analysis by Beacon Designer program, Free Edition (http://www.premierbiosoft.com/) and chromosome location confirmed by the in silico PCR (https://genome.ucsc.edu/). Primers characteristics, genes regions, and PCR conditions are illustrated in Table 2.

## 2.6 | Shh and Gli inhibition

Pre-osteoblasts ($25 \times 10^4$ cells) were seeded into 6-well plates in αMEM medium containing antibiotics (100 U/mL penicillin, 100 mg/mL streptomycin), ribonucleosides, deoxyribonucleosides, and 10% FBS (Nutricell). After 24 h of incubation at 37°C in a humidified atmosphere containing 5% $CO_2$, the cells were treated with 1 µM of Shh signaling antagonist, cyclopamine hydrate (C4116) or 5 µM of inhibitor of the transcriptional activity of Gli1, GANT61 (G8923). The control group was maintained in basal medium αMEM supplemented with ribonucleosides, deoxyribonucleosides and 10% FBS and antibiotics.

## 2.7 | Statistical analysis

All experiments were performed at three independent times in technical duplicate, totaling six replicas and the results were expressed as mean ± standard deviation. Statistical analysis was performed by Student's *t* test and analysis of variance (ANOVA one-way—Tukey) using GraphPad Prism 7 software (GraphPad Software Inc.).

# 3 | RESULTS

## 3.1 | rhBMP7 promotes hedgehog pathway activating during osteoblast differentiation

To determinate the involvement of Hh signaling pathway during BMP7-induced osteoblast differentiation, we performed qPCR analysis to assess the expression of *Ptch1*, *Sufu*, *Gli1*, and *Shh* genes. Initially, we validated the osteoblast differentiation model

10958355, 2024, 7, Downloaded from https://onlinelibrary.wiley.com/doi/10.1002/cbin.12161 by UNIP - Universidade Paulista, Wiley Online Library on [04/07/2025]. See the Terms and Conditions (https://onlinelibrary.wiley.com/terms-and-conditions) on Wiley Online Library for rules of use; OA articles are governed by the applicable Creative Commons License

**TABLE 1** Expression primers sequences and PCR cycle conditions.

| Gene (ID) | Primer | 5′– 3′ Sequence | Reactions' condicition | Product size (pb) |
|---|---|---|---|---|
| Gene expression | | | | |
| Runx 2 (12393) | Forward | GGA CGA GGC AAG AGT TTC A | 95°C—8 s; 58°C—8 s; 72°C—8 s | 249 |
| | Reverse | TGG TGC AGA GTT CAG GGA G | | |
| Osterix Sp7 (170574) | Forward | CCC TTC CCT CAC TCA TTT CC | 95°C—9 s; 63°C—9 s; 72°C—9 s | 427 |
| | Reverse | CAA CCG CCT TGG GCT TAT | | |
| Bsp (15891) | Forward | AGT GAA GGA AAG CGA CGA GG | 95°C—8 s; 58°C—8 s; 72°C—8 s | 218 |
| | Reverse | CTG TGG TTC CTT CTG CAC CT | | |
| Alp (11647) | Forward | CAT AGT CAC GGC CAG TCC TC | 95°C—8 s; 63°C—8 s; 72°C—8 s | 179 |
| | Reverse | AGT CTC TGC AAT TGG GTG GG | | |
| Shh (20423) | Forward | AGC GAC TGC GAA ATA AGG AA | 95°C—8 s; 59°C—8 s; 72°C—8 s | 234 |
| | Reverse | GCC AGG AGA GGA GAA AAA CA | | |
| Sufu (24069) | Forward | TGA AAA GAT GCT TGG TGC TG | 95°C—15 s; 60°C—30 s; 72°C—30 s | 155 |
| | Reverse | TCC CCA GAG CCT TGT AGA GA | | |
| Patch 1 (19206) | Forward | TGT GTG CAT GTG ACT TTC CA | 95°C—15 s; 60°C—30 s; 72°C—30 s | 152 |
| | Reverse | CCA GCA TCA CGA CAG AAA AA | | |
| Gli 1 (14632) | Forward | GAA GGA ATT CGT GTG CCA TT | 95°C—15 s; 59°C—8 s; 72°C—8 s | 148 |
| | Reverse | GCG TCT TGA GGT TTT CAA GG | | |
| Dhh (11461) | Forward | CTT CGG TCC AGT GGT TGT TT | 95°C—15 s; 58°C—30 s; 72°C—30 s | 175 |
| | Reverse | TAC ATG CCC ATC CCT AGC TC | | |
| Ihh (14433) | Forward | CGT GCA TTG CTC TGT CAA GT | 95°C—15 s; 63°C—30 s; 72°C—30 s | 230 |
| | Reverse | CTC GAT GAC CTG GAA AGC TC | | |
| Dnmt1 (13433) | Forward | CCT TTG TGG GAA CCT GGA A | 95°C—15 s; 63°C—30 s; 72°C—30 s | 178 |
| | Reverse | CTG TCG TCT GCG GTG ATT | | |
| Dnmt3a (13435) | Forward | GAG GGA ACT GAG ACC CCA C | 95°C—15 s; 63°C—30 s; 72°C—30 s | 216 |
| | Reverse | CTG GAA GGT GAG TCT TGG CA | | |
| Dnmt3b (13436) | Forward | AGC GGG TAT GAG GAG TGC AT | 95°C—15 s; 63°C—30 s; 72°C—30 s | 72 |
| | Reverse | GGG AGC ATC CTT CGT GTC TG | | |
| Tet1 (52463) | Forward | GAG CCT GTT CCT CGA TGT GG | 95°C—15 s; 65°C—30 s; 72°C—30 s | 202 |
| | Reverse | CAA ACC CAC CTG AGG CTG TT | | |
| Tet2 (214133) | Forward | AAC CTG GCT ACT GTC ATT GCT CCA | 95°C—15 s; 65°C—30 s; 72°C—30 s | 182 |
| | Reverse | ATG TTC TGC TGG TCT CTG TGG GAA | | |
| Tet3 (193348) | Forward | GTC TCC CCA GTC CTA CCT CCG | 95°C—15 s; 58°C—30 s; 72°C—30 s | 136 |
| | Reverse | GTC AGT GCC CCA CGC TTC A | | |
| β-actin (11461) | Forward | TCT TGG GTA TGG AAT CCT GTG | 95°C—15 s; 58°C—30 s; 72°C—30 s | 82 |
| | Reverse | AGG TCT TTA CGG ATG TCA ACG | | |
| Gapdh (14433) | Forward | CCG CAG CGA GGA GTT TCT C | 95°C—15 s; 63°C—30 s; 72°C—30 s | 530 |
| | Reverse | GAG CTA AGC TCA GGC TGT TCC A | | |

10958355, 2024, 7, Downloaded from https://onlinelibrary.wiley.com/doi/10.1002/cbin.12161 by UNIP - Universidade Paulista, Wiley Online Library on [04/07/2025]. See the Terms and Conditions (https://onlinelibrary.wiley.com/terms-and-conditions) on Wiley Online Library for rules of use; OA articles are governed by the applicable Creative Commons License

**TABLE 2** Shh signaling members gene-related methylation primer sequences and qPCR conditions.

| Gene (ID) | Primer | 5'- 3' Sequence | Reaction's condition | Product size (pb) | CpG location |
|---|---|---|---|---|---|
| Shh (20423) | Forward | AGG AAG GTG AGG AAG TCG CT | 95°C–15 s; 60°C–30 s; 72°C–30 s | 244 | chr 4 28784319-28785746 (site 5) |
| | Reverse | CAC ACA CAC ACG CTC GTA CA | | | |
| Ptch1 (19206) | Forward | GGA TCC CAA GGA GGA AGA AG | 95°C–15 s; 60°C–30 s; 72°C–30 s | 217 | chr 13 63664549-63667490 (site6) |
| | Reverse | ATG GCC TCG GCT GGT AAC | | | |
| Sufu (24069) | Forward | CTC TAC CCT CCC GGG TTC T | 95°C–15 s; 60°C–30 s; 72°C–30 s | 214 | chr 19 46450187-46450655 (site 4) |
| | Reverse | GAC GAT AGC GGT AAC CTG GA | | | |
| Gli (14632) | Forward | AGC GAC TGC GAA ATA AGG AA | 95°C–15 s; 60°C–30 s; 72°C–30 s | 380 | chr 10 127339344-127339723 (site 5) |
| | Reverse | GCC AGG AGA GGA GAA AAA CA | | | |

by evaluating osteoblastic gene markers. Notably, at day 7, the expression of *Runx2*, *Osterix*, *Bsp*, and *Alp* genes significantly increased in response to rhBMP7 (Figure 1). Furthermore, at day 14, *Bsp* and *Alp* genes remained elevated compared to the control. In contrast, there was a decrease in Runx2 gene expression, accompanied by a significant increase in *Alp* at day 21 (Figure 1a–d). In terms of Hh signaling involvement during osteoblast differentiation, our data demonstrates a significant involvement of both *Shh* ligand and *Ptch1* gene signaling members at 7 days, with *Sufu* continuing to exhibit higher levels at both 14 and 21 days (Figure 1e–h). This suggests that *Shh* plays a crucial role during the early stages of osteoblast differentiation, possibly correlating with mechanisms capable of activating osteogenic transcription factors, such as *Runx2* and *Osterix*.

### 3.2 | rhBMP7 signaling affects the messenger RNA (mRNA) expression of genes involved with the balance of DNA methylation processes

Thereafter, epigenetic machinery was partially evaluated and our data shows a significant modulation of genes related with the global DNA-methylation balance (Figure 2). At day 7, *Dnmt1* gene was significantly higher (40-fold changes) and this profile was significantly decreased at days 14 and 21 (Figure 2a). *Dnmt3A* was significantly lower along of the 21 days (Figure 2b), while *Dnmt3B* was significantly higher at day 21. Additionally, we have also focused on the ten-eleven translocation (TET) genes encoding enzymes oxidize 5-methylcytosines (5-meC) (Figure 2d–f). Our data shows there is no significant changes on *Tet1* gene expression (Figure 2d), while *Tet2* gene was significantly higher at day 7 (Figure 2e) and *Tet3* was significantly lower at day 21 (Figure 2f).

### 3.3 | rhBMP7 promotes significant changes in CpG methylation of hedgehog signaling pathway related members

Overall, the Figure 3 brings the panorama of the CpG methylation of Hh signaling pathway members. Regarding the Shh (ligand), our data shown a maintenance of their methylation profile up to 21 days, with higher levels of 5-meC than 5-hmeC (Figure 3a–c). In turn, *Ptch1* gene expression was epigenetically modulated along of the rhBMP7-induced pObs differentiation. Although 5-meC pattern is maintained high up to day 21 and without significances in comparison with the unchallenged cell (Figure 3a–f), the profile of 5-hmeC was significantly decreased at day 14, maybe contributing with the methylation pattern of *Ptch1* promoter (Figure 3c). Additionally, *Sufu* was also evaluated regarding their CpG methylation promoter (Figure 3g–i). Significantly, our data shows an positive relation at days 14 and 21, suggesting a significant methylation status of its promoter (Figure 3h,i).

10958355, 2024, 7, Downloaded from https://onlinelibrary.wiley.com/doi/10.1002/cbin.12161 by UNIP - Universidade Paulista, Wiley Online Library on [04/07/2025]. See the Terms and Conditions (https://onlinelibrary.wiley.com/terms-and-conditions) on Wiley Online Library for rules of use; OA articles are governed by the applicable Creative Commons License

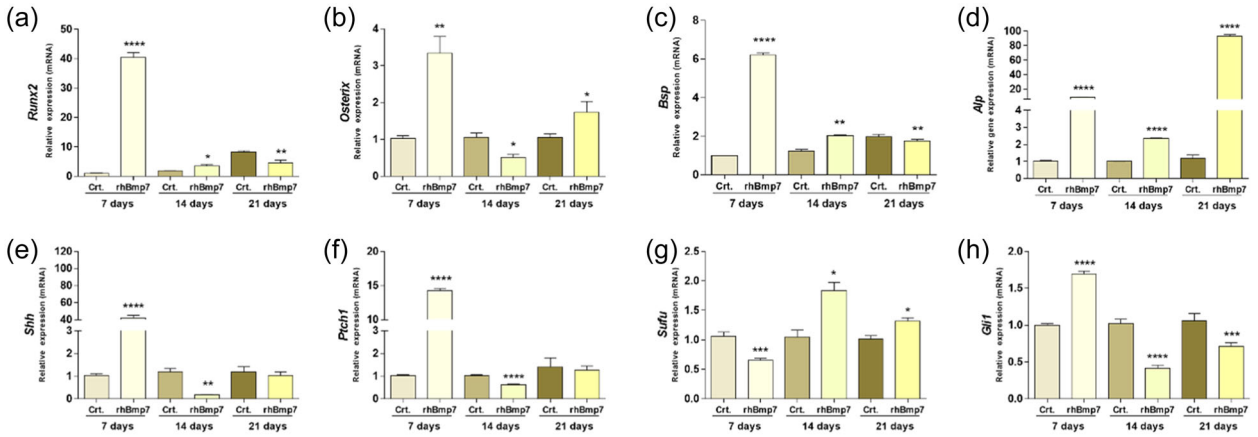


**FIGURE 1** Sonic hedgehog signaling is finely modulated during osteoblast differentiation. MC3T3-E1 cells were treated with rhBMP7. Total mRNA was isolated to allow the expression of *Runx2* (a), *Osterix* (b), *Bsp* (c), *Alp* (d), *Shh* (e), *Ptch1* (f), *Sufu* (g) and *Gli1* (h) by real-time RTqPCR. The values were normalized to *β-actin* and *Gapdh*. Analyzes were performed using a *t*-test between the control and treated groups at each time point and the results were expressed as mean ± standard deviation. The experiment was carried out in triplicate, with technical duplicate ($n = 6$). Significances were considered when $^{*}p < .05$, $^{**}p < .01$, $^{***}p < .001$, and $^{****}p < 0.0001$. mRNA, messenger RNA.

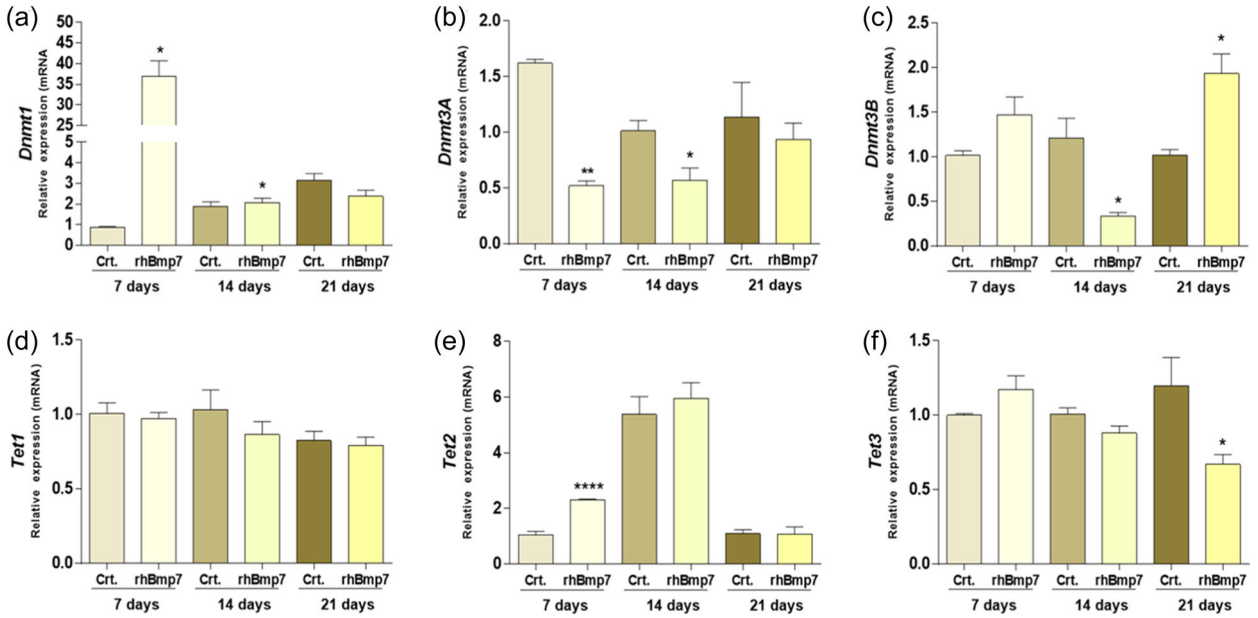


**FIGURE 2** Effect of rhBMP7 on the transcriptional profile of genes related with DNA methylation balance. MC3T3-E1 cells were treated with rhBMP7 (100 ng/mL). Total mRNA was isolated to allow the expression of *Dmnt1* (a), *Dnmt3A* (b), *Dmnt3B* (c), *Tet1* (d), *Tet2* (e), and *Tet3* (f) by real-time RTqPCR. The values were normalized to *β-actin* and *Gapdh*. The experiment was carried out in triplicate with technical duplicate ($n = 6$) and the analyzes were performed using a *t*-test between the control and treated groups at each time point and the results were expressed as mean ± standard deviation. Significances were considered when $^{*}p < .05$, $^{**}p < .01$, $^{***}p < .001$, and $^{****}p < .0001$. mRNA, messenger RNA.

Finally, *Gli1* promoter methylation balance was also considered in this study, and the results reveal a significant decrease of methylation/hydroxymethylation ratio at days 14 and 21, suggesting its importance during osteoblast differentiation. Importantly, we have shown a positive correlation value highlighting the higher expression of *Gli1* transcripts (mRNA) profile with concomitant decrease of gene promoter methylation (Figure 4c), presenting a Pearson's product above $r > .6$ for *Ptch1* and *Gli* up to14 days.

### 3.4 | Suppression of hedgehog signaling compromises osteoblastic differentiation

Based on the aforementioned results, which emphasize the significant activation of the Hh pathway in response to rhBMP7, we conducted a more in-depth exploration to comprehend its role in osteoblast differentiation by employing classical Hh inhibitors: GANT-61, a Gli1 antagonist, and cyclopamine (Cyclo), a potent inhibitor of the Shh signaling pathway. In the group where

10983355, 2024, 7, Downloaded from https://onlinelibrary.wiley.com/doi/10.1002/cbin.12161 by UNIP - Universidade Paulista, Wiley Online Library on [04/07/2025]. See the Terms and Conditions (https://onlinelibrary.wiley.com/terms-and-conditions) on Wiley Online Library for rules of use; OA articles are governed by the applicable Creative Commons License

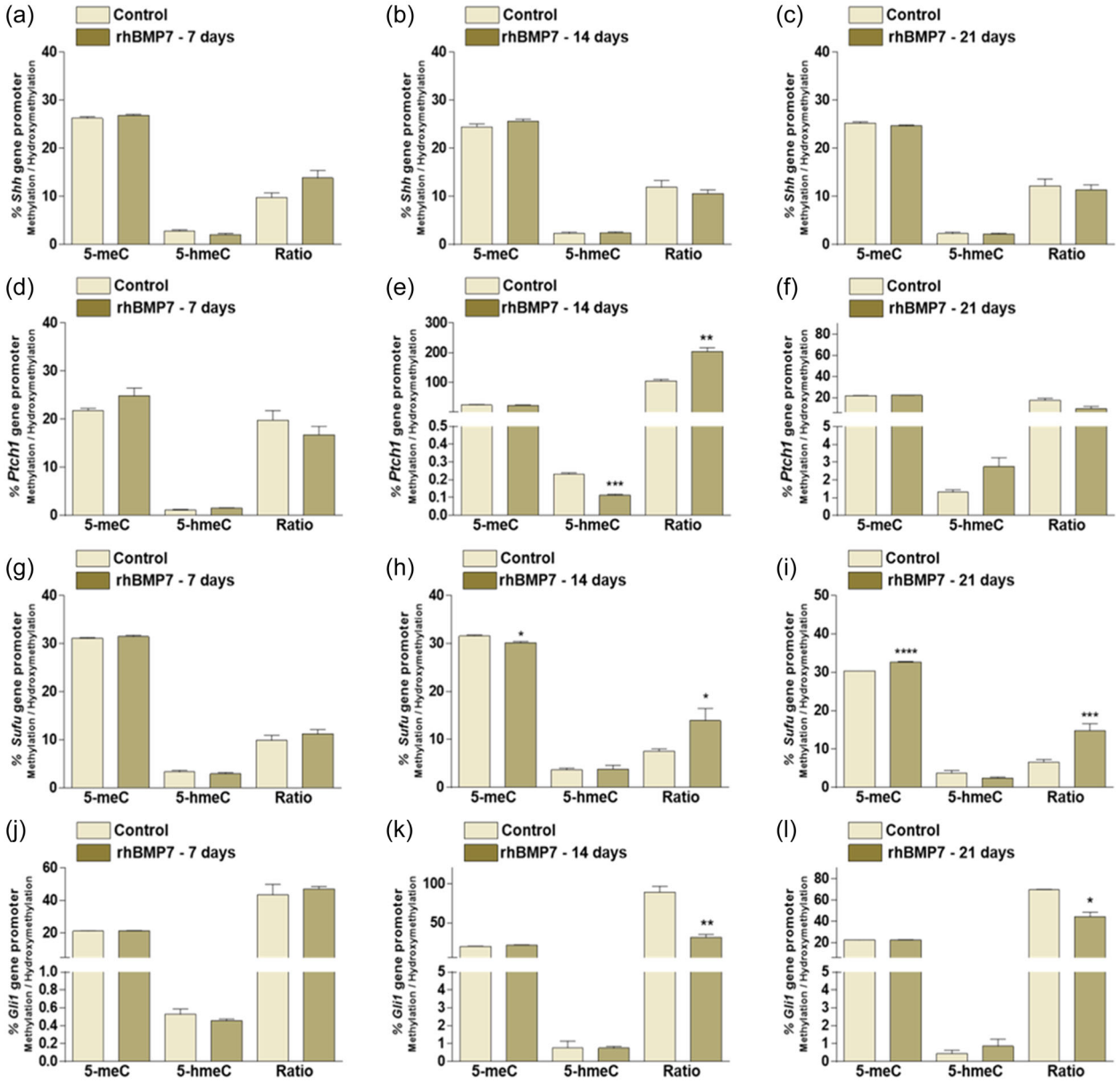


**FIGURE 3** Effect of rhBMP7 on CpG methylation of hedgehog signaling pathway members. *Shh* (a–c), *Ptch1* (d–f), *Sufu* (g–i) and *Gli1* (j–l) gene promoter methylation balance. The DNA methylation status of the hedgehog pathway member genes based on the qPCR data obtained after 7, 14, and 21 days of differentiation with 100 ng/mL hrBMP7 is shown after it is normalized. The relative levels were determined using the cycle threshold (Ct) method and the methylation results are presented as *Hpa*II levels—*Msp*I levels/control levels and the hydroxymethylation results are presented as *Msp*I levels-control levels. Results were represented as mean ± standard deviation of three independent experiments with technical duplicate ($n = 6$). *$p < .05$, **$p < .01$, ***$p < .001$, and ****$p < .0001$.

inhibition was carried out by Cyclo, there is an increase in the expression of all genes associated with this pathway (Figure 5a–d). In contrast, the group treated with GANT-61 exhibited increased expression only in *Shh* and *Sufu* when compared to the control (Figure 5a and 5c). Taken these data into account, it is reasonable suggest that Hh signaling plays a synergistic role with BMP signaling, potentially establishing an autocrine loop following rhBMP7 activation and this synergy could enhance the crucial signaling pathway responsible for driving the expression of osteoblastic gene markers.

Upstream inhibition of the signaling by Cyclo led to higher expressions of *Runx2*, *Bsp*, and *Alp* (Figure 5e and 5g,h), while GANT-61 seemed to primarily promote the expression of *Osterix* (Figure 5e,f). Interestingly, the inhibition of *Gli1* appears to impair the expression of *Bsp* and *Alp* genes in response to rhBMP7, suggesting the potential involvement of *Gli1* only in the final stages of osteoblastic differentiation triggered by BMP7 (Figure 5g,h). Also on this regard, we consider to evaluate the involvement of other signaling pathway ligands: Indian (Ihh) and desert (Dhh) hedgehogs (Figure 6). We highlight here the increase

10958355, 2024, 7, Downloaded from https://onlinelibrary.wiley.com/doi/10.1002/cbin.12161 by UNIP - Universidade Paulista, Wiley Online Library on [04/07/2025]. See the Terms and Conditions (https://onlinelibrary.wiley.com/terms-and-conditions) on Wiley Online Library for rules of use; OA articles are governed by the applicable Creative Commons License

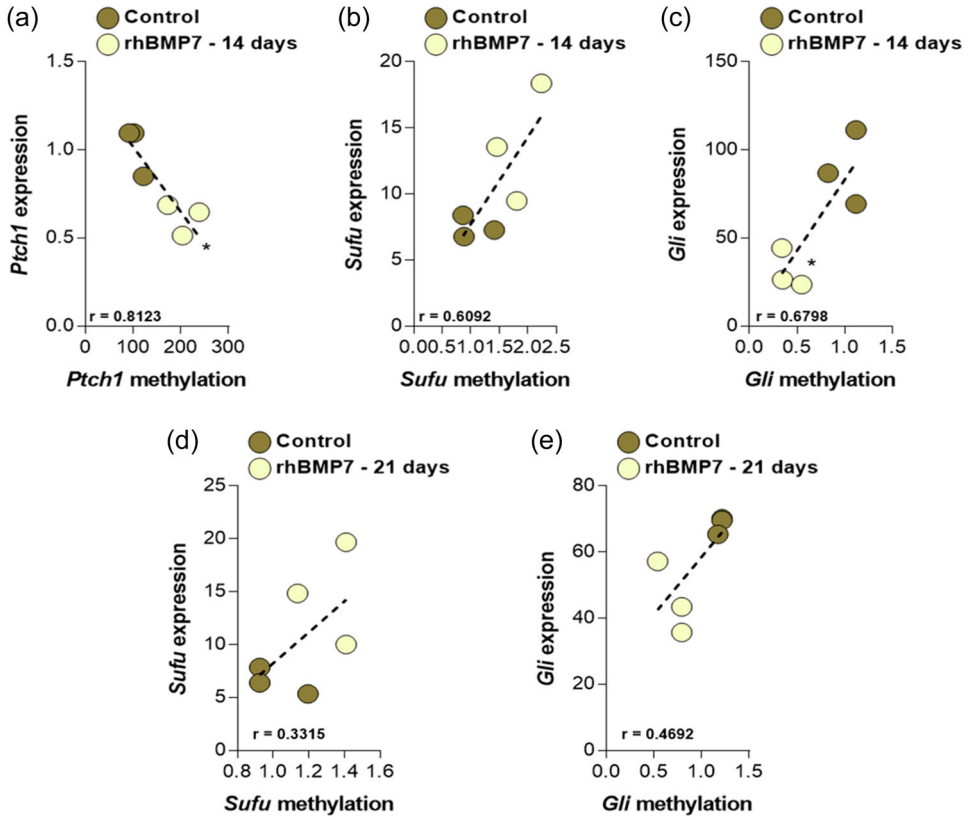


**FIGURE 4** Correlation of the efficiency of the epigenetic machinery in modulating gene expression. Correlation analysis between gene promoter DNA methylation/hydroxymethylation pattern and gene expression of *Ptch1*, *Sufu*, and *Gli1* in 14 (a–c) and *Sufu* and *Gli1* in 21 (d, e) days. Significant positive correlation between $r = .683$ and 1.

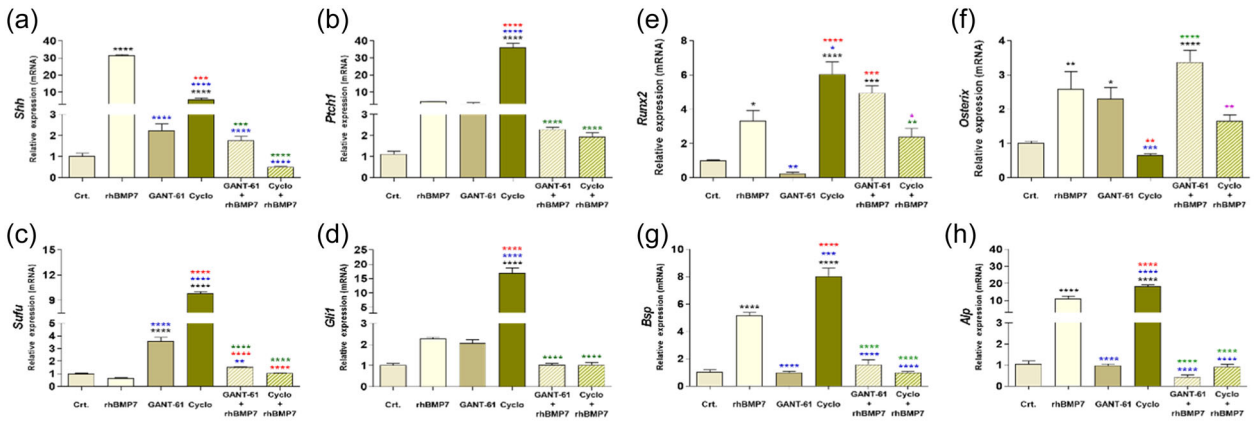


**FIGURE 5** Effects of Shh signaling-motived inhibitors in osteoblast gene markers. MC3T3-E1 cells were treated with rhBMP7, GANT-61, Cyclo, rhBMP7+GANT-61 and rhBMP7+Cyclo during 7 days. Total RNA was isolated to allow gene expression of *Shh* (a), *Ptch1* (b), *Sufu* (c), *Gli1* (d), *Runx2* (e), *Osterix* (f), *Bsp* (g), and *Alp* (h), measured by RTqPCR. The values were normalized to both β-actin and Gapdh and expressed as fold-change increase based on control with means ($n = 6$) ± *SE*, after analysis of one-way ANOVA (performed by Tukey). Significances are highlighted with asterisk, as follows: *$p < .05$, **$p < .01$, ***$p < .001$, and ****$p < .0001$ (differences between groups: *control; *rhBMP7, * Gant-61, * Cyclo, * Gant-61+rhBMP7—black is compared with control, blue is compared with rhBMP7, red is compared with Gant-61, green is compared with Cyclo and purple compared with Gant61+rhBMP7). ANOVA, analysis of variance.

in the expression of these genes at 14 and 21 days when treated with rhBMP7 (Figure 6a,b). When treating the groups with the GANT-61 and Cyclo inhibitors, we observed that only the group that received the Cyclo inhibitor showed high expression (Figure 6c). The events noted here have been summarized in Figure 7, illustrating our main findings during the investigation of the synergies between rhBMP7 and the Hh pathway during the differentiation of the osteobalsts.

10958355, 2024, 7, Downloaded from https://onlinelibrary.wiley.com/doi/10.1002/cbin.12161 by UNIP - Universidade Paulista, Wiley Online Library on [04/07/2025]. See the Terms and Conditions (https://onlinelibrary.wiley.com/terms-and-conditions) on Wiley Online Library for rules of use; OA articles are governed by the applicable Creative Commons License

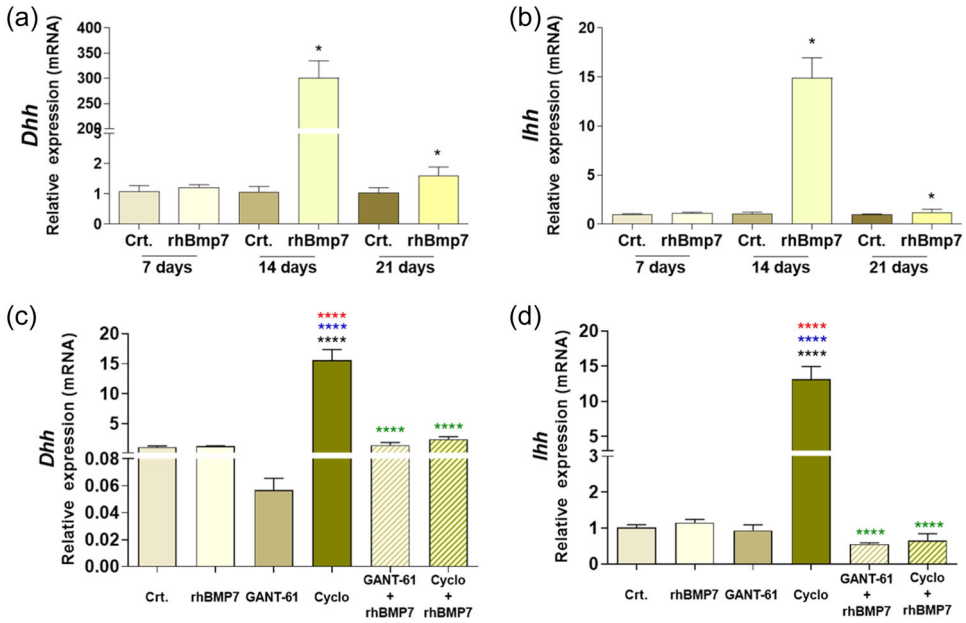


**FIGURE 6** Involvement of Dhh and Ihh genes during BMP7-induced osteoblastic differentiation and their activities in response to inhibitors related to Hh signaling. MC3T3-E1 cells were treated with rhBMP7 for 7, 14, and 21 days. Total mRNA was isolated to allow expression of Dhh (a), Ihh (b) analyzed by *t*-test. Subsequently, MC3T3-E1 cells were treated with rhBMP7, GANT-61, Cyclo, rhBMP7+GANT-61 and rhBMP7+Cyclo for 7 days. Total mRNA was isolated to allow expression of the Dhh (c) and Ihh (d) genes by real-time RTqPCR. Values were normalized for β-actin and Gapdh and expressed as increased variance based on control with means ($n = 6$) ± *SE* after analysis by one-way ANOVA (performed by Tukey). Significance was considered when $^{*}p < .05$, $^{**}p < .01$, $^{***}p < .001$, and $^{****}p < .0001$ (differences between groups: *control; *rhBMP7, * Gant-61, * Cyclo, * Gant-61+rhBMP7—black is compared with control, blue is compared with rhBMP7, red is compared with Gant-61, green is compared with Cyclo and purple compared with Gant61+rhBMP7). ANOVA, analysis of variance; mRNA, messenger RNA.

## 4 | DISCUSSION

To enhance our understanding of the molecular mechanisms driving preosteoblast (pObs) differentiation, we focused on inducing osteoblast differentiation in vitro using the trophic and well-established molecule, rhBMP7 (Carreira et al., 2015). Initially, we demonstrated the pivotal role of rhBMP7 in promoting complete osteoblast differentiation by evaluating classical osteogenic gene markers, such as Runx2 and Osterix, Bone Sialoprotein (BSP) and Alkaline Phosphatase (ALP). Both BSP and ALP serve together as biomarkers related to the late stages of osteoblast differentiation and are responsible for driving mineralization in vitro. Bone morphogenetic proteins (BMPs) and members of the hedgehog family are intricately linked to morphogenetic signaling pathways in vertebrates, playing a crucial role in distinguishing cell fate during differentiation. We validated and further explored this biological model for pObs differentiation to investigate whether this mechanism involves hedgehog (Hh) signaling pathway members. While the importance of Sonic hedgehog (Shh) signaling in the osteoblastic phenotype, particularly in the transition from osteoblasts to osteocytes (da Costa Fernandes et al., 2023; Marumoto et al., 2017), is evident the regulatory mechanism remains unclear even considering the interplay between them.

Evaluating hedgehog (Hh) signaling pathway members, we noted higher levels of both the Shh ligand and the patched 1 (Ptch1) genes in preosteoblasts (pObs) without any treatment, suggesting constitutive expression in osteoblasts. Contextualizing this elevated Shh expression, it seems linked to autocrine and paracrine signaling, impacting the partially differentiated phenotype of pObs. This may act as an initial factor in triggering osteoblast differentiation (da S. Feltran, Bezerra, da Costa Fernandes, Ferreira, and Zambuzzi, 2019) and this prompt us to investigate the epigenetic machinery to better understand the regulatory mechanism driving the osteogenic phenotype. Important to mention that the pattern of DNA methylation at cytosine bases in the genome is intricately connected to gene expression, and irregularities in DNA methylation are frequently observed in diseases. Exceptions to the widespread genomic methylation can be found in gene regulatory regions, such as CpG-rich promoter elements (known as CpG islands), and active enhancers, often associated with a low DNA methylation profile (Rasmussen & Helin, 2016). Thus, genes encoding methylation metabolism-related enzymes were investigated during osteoblast differentiation—on day 7, our findings indicate a notable increase in the expression of *Dnmt1* and *Tet2*, whereas the *Dnmt3A* and *3B* genes were downregulated until day 14, while *Dnmt3B* exhibited an increase—on day 21 in response to BMP.

Thereafter, more specific epigenetic changes were evaluated by examining the expression of gene-specific promoters associated with the hedgehog (Hh) pathway. Our data demonstrate that *Sufu*, *Ptch1*, and *Gli1* genes underwent precise modulation through epigenetic

10958355, 2024, 7, Downloaded from https://onlinelibrary.wiley.com/doi/10.1002/cbin.12161 by UNIP - Universidade Paulista, Wiley Online Library on [04/07/2025]. See the Terms and Conditions (https://onlinelibrary.wiley.com/terms-and-conditions) on Wiley Online Library for rules of use; OA articles are governed by the applicable Creative Commons License

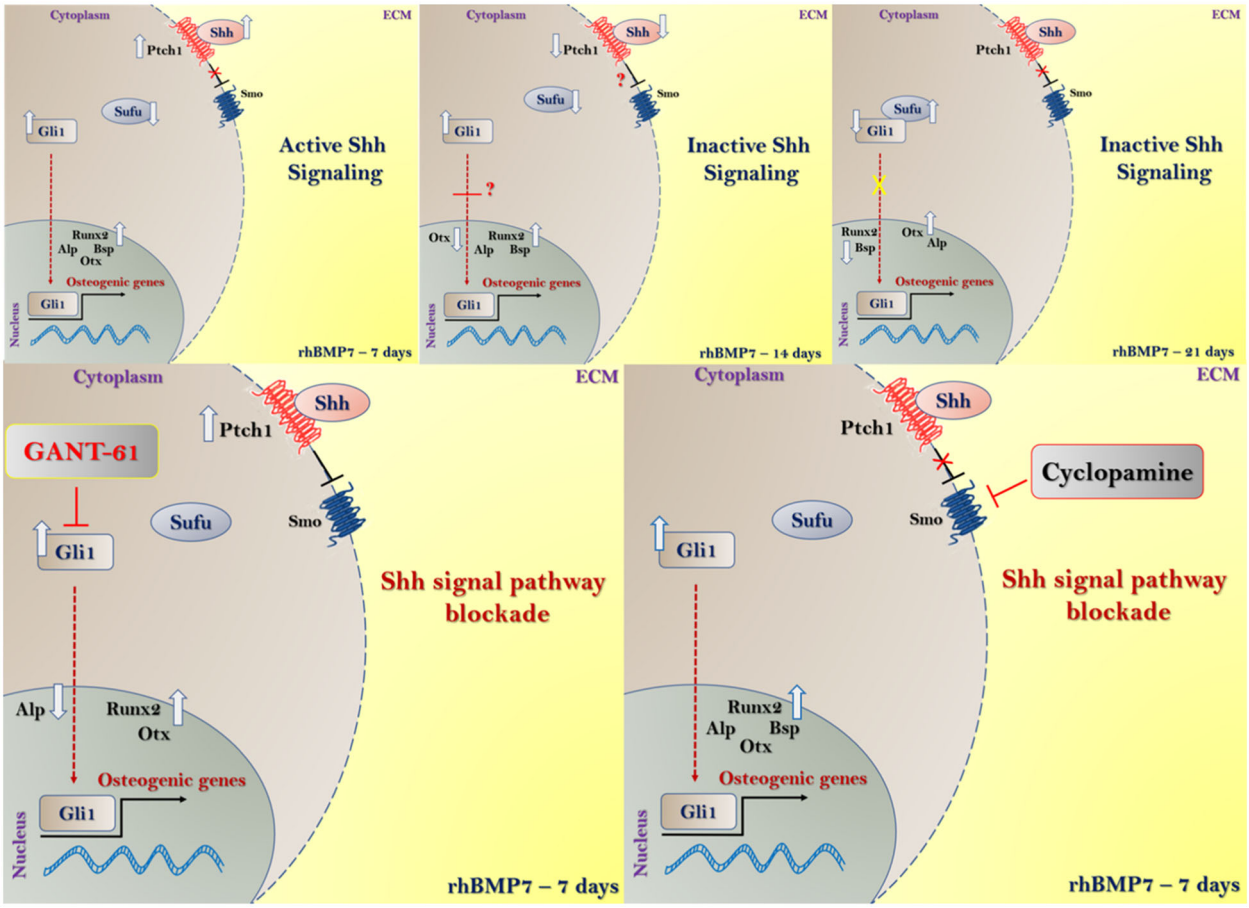


**FIGURE 7** Interplay of BMP7 and hedgehog signaling in osteoblast differentiation. BMP-7 critically induces osteoblast differentiation through Sonic hedgehog (Shh) signaling, promoting the expression of key biomarkers during the early (7 days) and late (14 and 21 days) stages of differentiation. Initially, Shh pathway activation upregulates Ptch1 and Gli1 while downregulating Sufu, facilitating the early expression of differentiation biomarkers like Runx2, Osterix (Otx), Alkaline phosphatase (Alp), and Bone sialoprotein (Bsp). As differentiation progresses (14 and 21 days), mineralization commences, reducing Shh availability and incrementally increasing Sufu expression, which inhibits Gli1, diminishing early markers and sustaining late-stage markers' expression. To dissect Shh role, osteoblasts were treated with BMP7 and classical Shh pathway inhibitors: Gli1 antagonist (GANT-61) and cyclopamine (Cyclo), a robust Shh pathway inhibitor. Gli1 inhibition downregulated Alp while enhancing Runx2 and Otx expression, implicating Gli1's role in response to BMP7. Conversely, cyclopamine treatment increased Runx2 and Otx expression, suggesting positive feedback mechanisms are at play.

markers, establishing a pattern of methylation (5-meC) rather than hydroxymethylation (5-hmeC). An exception was noted for *Gli1* on both days 14 and 21, where its gene promoter displayed hypo-methylation, promoting its expression. Further analyses, utilizing Pearson correlation for Ptch1 and Gli1, provide support for the involvement of these genes in regulating Hh-related signaling and downstream signals during osteoblast differentiation. So far, TET enzymes have been recognized as crucial in oxidizing 5-methylcytosines (5-meC) to 5-hydroxymethylcytosines (5-hmeC), facilitating locus-specific reversal of DNA methylation, while *Ptch1* and *Gli1* genes are also implicated in osteoblast differentiation (Hashimoto et al., 2014; He et al., 2011; Ito et al., 2011, 2013).

Finally, to validate our hypothesis supporting that Shh-related signaling contributes to the osteoblastic phenotype, we employed chemically designed molecules to inhibit Smo and Gli1, namely cyclopamine and GANT-61, respectively. Our data reveals a potential synergism between BMP7-related signaling and the Shh signaling pathway, possibly mediated by BMP7 inducing the expression of Shh in an autocrine loop, as it has been suggested earlier during bone development (Yamaguchi et al., 2000). Additionally, downstream signaling upon BMP activation may involve Gli1 and Shh signaling to synergistically promote osteogenic gene markers expression such as *Alp* and *Bsp*. This synergistic effect is shown by the significant increase in the expression of *Shh* (ligand, ~30-fold) and *Gli1* (~3-fold) induced by rhBMP7 compared to unchallenged cells. Notably, *Alp* expression deserve attention—we observed a significant increase in the *Alp* gene in challenged cells (~100-fold) at 21 days, and its functionality is significantly hindered when cells are pre-treated with GANT-61, a Gli1 inhibitor. This suggests significance of Gli1 in activating the *Alp* gene in response to rhBMP7, either by acting directly as a transcription factor or interacting upstream with the epigenetic machinery.

10958355, 2024, 7, Downloaded from https://onlinelibrary.wiley.com/doi/10.1002/cbin.12161 by UNIP - Universidade Paulista, Wiley Online Library on [04/07/2025]. See the Terms and Conditions (https://onlinelibrary.wiley.com/terms-and-conditions) on Wiley Online Library for rules of use; OA articles are governed by the applicable Creative Commons License

Altogether, our findings support the idea of epigenetic machinery is required during rhBMP7-induced osteogenic phenotype, thereby influencing the activity of Hh-related genes. Furthermore, the impact of Hh ligands, especially Shh, in potentialize the effects of rhBMP7 signaling, reinforcing the commitment of osteogenic signaling. This contribution is particularly pronounced in the late phase of osteoblast differentiation, where Gli1 seems to synergize with dual upstream signals, guiding the activities of the Alp and Bsp genes in a non-canonical manner. Epigenetic studies that focus on transcript profiles can thus reveal how external factors like BMP7 and hedgehog (Hh) signaling can lead to enduring changes in gene expression, driving the fate of progenitor cells towards a mature osteoblastic lineage and looking for potential pharmacological development of drugs able to treat bone disorders.

## ACKNOWLEDGMENTS

Fundação de Amparo à Pesquisa do Estado de São Paulo—FAPESP (FAPESP: 2019/26854-2; 2014/22689-3; 2016/01139-0) and Conselho Nacional de Desenvolvimento Científico e Tecnológico (CNPq—Bolsa Produtividade em Pesquisa, 314166/2021-1 and 301498/2022-9).

## CONFLICT OF INTEREST STATEMENT

The authors declare no conflicts of interest.

## DATA AVAILABILITY STATEMENT

The data that support the findings of this study are available from the corresponding author upon reasonable request.

## ORCID

*Georgia da Silva Feltran* http://orcid.org/0000-0002-5743-5182
*Willian F. Zambuzzi* http://orcid.org/0000-0002-4149-5965

## REFERENCES

Assis, R. I. F., Schmidt, A. G., Racca, F., da Silva, R. A., Zambuzzi, W. F., Silvério, K. G., Nociti, F. H., Pecorari, V. G., Wiench, M., & Andia, D. C. (2021). DNMT1 inhibitor restores RUNX2 expression and mineralization in periodontal ligament cells. *DNA and Cell Biology*, *40*(5), 662–674. https://doi.org/10.1089/dna.2020.6239

Bae, W.-J., Auh, Q.-S., Lim, H.-C., Kim, G.-T., Kim, H.-S., & Kim, E.-C. (2016). Sonic hedgehog promotes cementoblastic differentiation via activating the BMP pathways. *Calcified Tissue International*, *99*(4), 396–407. https://doi.org/10.1007/s00223-016-0155-1

Bai, C. B., Auerbach, W., Lee, J. S., Stephen, D., & Joyner, A. L. (2002). Gli2, but not Gli1, is required for initial Shh signaling and ectopic activation of the Shh pathway. *Development*, *129*(20), 4753–4761.

Caradu, C., Guy, A., James, C., Reynaud, A., Gadeau, A.-P., & Renault, M.-A. (2018). Endogenous Sonic Hedgehog limits inflammation and angiogenesis in the ischaemic skeletal muscle of mice. *Cardiovascular Research*, *114*, 759–770. https://doi.org/10.1093/cvr/cvy017

Carreira, A. C. O., Zambuzzi, W. F., Rossi, M. C., Astorino Filho, R., Sogayar, M. C., & Granjeiro, J. M. (2015). Bone morphogenetic proteins: promising molecules for bone healing, bioengineering, and regenerative Medicine. *Vitamins and Hormones*, *99*, 293–322. https://doi.org/10.1016/bs.vh.2015.06.002

da Costa Fernandes, C. J., Ferreira, M. R., & Zambuzzi, W. F. (2023). Cyclopamine targeting hedgehog modulates nuclear control of the osteoblast activity. *Cells & Development*, *174*, 203836. https://doi.org/10.1016/j.cdev.2023.203836

Ergun, S., & Oztuzcu, S. (2015). Oncocers: ceRNA-mediated cross-talk by sponging miRNAs in oncogenic pathways. *Tumor Biology*, *36*(5), 3129–3136. https://doi.org/10.1007/s13277-015-3346-x

Eslaminejad, M. B., Fani, N., & Shahhoseini, M. (2013). Epigenetic regulation of osteogenic and chondrogenic differentiation of mesenchymal stem cells in culture. *Cell Journal*, *15*(1), 1–10.

Ferreira, R. S., Assis, R. I. F., Feltran, G. S., do Rosário Palma, I. C., Françoso, B. G., Zambuzzi, W. F., Andia, D. C., & da Silva, R. A. (2022). Genome-wide DNA (hydroxy) methylation reveals the individual epigenetic landscape importance on osteogenic phenotype acquisition in periodontal ligament cells. *Journal of Periodontology*, *93*(3), 435–448. https://doi.org/10.1002/JPER.21-0218

Hashimoto, H., Pais, J. E., Zhang, X., Saleh, L., Fu, Z.-Q., Dai, N., Corrêa, I. R., Zheng, Y., & Cheng, X. (2014). Structure of a Naegleria Tet-like dioxygenase in complex with 5-methylcytosine DNA. *Nature*, *506*(7488), 391–395. https://doi.org/10.1038/nature12905

He, Y.-F., Li, B.-Z., Li, Z., Liu, P., Wang, Y., Tang, Q., Ding, J., Jia, Y., Chen, Z., Li, L., Sun, Y., Li, X., Dai, Q., Song, C.-X., Zhang, K., He, C., & Xu, G.-L. (2011). Tet-mediated formation of 5-carboxylcytosine and its excision by TDG in mammalian DNA. *Science*, *333*(6047), 1303–1307. https://doi.org/10.1126/science.1210944

Ito, S., Shen, L., Dai, Q., Wu, S. C., Collins, L. B., Swenberg, J. A., He, C., & Zhang, Y. (2011). Tet proteins can convert 5-methylcytosine to 5-formylcytosine and 5-carboxylcytosine. *Science*, *333*(6047), 1300–1303. https://doi.org/10.1126/science.1210597

James, A. W., Leucht, P., Levi, B., Carre, A. L., Xu, Y., Helms, J. A., & Longaker, M. T. (2010). Sonic Hedgehog influences the balance of osteogenesis and adipogenesis in mouse adipose-derived stromal cells. *Tissue engineering. Part A*, *16*(8), 2605–2616. https://doi.org/10.1089/ten.TEA.2010.0048

Kiuru, M., Solomon, J., Ghali, B., van der Meulen, M., Crystal, R. G., & Hidaka, C. (2009). Transient overexpression of sonic hedgehog alters the architecture and mechanical properties of trabecular bone. *Journal of Bone and Mineral Research*, *24*(9), 1598–1607. https://doi.org/10.1359/jbmr.090313

Lappalainen, T., & Greally, J. M. (2017). Associating cellular epigenetic models with human phenotypes. *Nature Reviews Genetics*, *18*(7), 441–451. https://doi.org/10.1038/nrg.2017.32

Li, T., Zhang, C., Hassan, S., Liu, X., Song, F., Chen, K., Zhang, W., & Yang, J. (2018). Histone deacetylase 6 in cancer. *Journal of Hematology & Oncology*, *11*(1), 111. https://doi.org/10.1186/s13045-018-0654-9

Liu, L., Hu, K., Feng, J., Wang, H., Fu, S., Wang, B., Wang, L., Xu, Y., Yu, X., & Huang, H. (2021). The oncometabolite R-2-hydroxyglutarate dysregulates the differentiation of human mesenchymal stromal cells via inducing DNA hypermethylation. *BMC Cancer*, *21*(1), 36. https://doi.org/10.1186/s12885-020-07744-x

Lopez-Rios, J. (2016). The many lives of SHH in limb development and evolution. *Seminars in Cell & Developmental Biology*, *49*, 116–124. https://doi.org/10.1016/j.semcdb.2015.12.018

Lorenzen, J. M., & Thum, T. (2016). Long noncoding RNAs in kidney and cardiovascular diseases. *Nature Reviews. Nephrology*, *12*(6), 360–373. https://doi.org/10.1038/nrneph.2016.51

Mak, K. K., Bi, Y., Wan, C., Chuang, P.-T., Clemens, T., Young, M., & Yang, Y. (2008). Hedgehog signaling in mature osteoblasts regulates bone formation and resorption by controlling PTHrP and RANKL expression. *Developmental Cell*, *14*(5), 674–688. https://doi.org/10.1016/j.devcel.2008.02.003

Marini, F., Cianferotti, L., & Brandi, M. (2016). Epigenetic mechanisms in bone biology and osteoporosis: Can they drive therapeutic choices? *International Journal of Molecular Sciences*, *17*(8), 1329. https://doi.org/10.3390/ijms17081329

10958355, 2024, 7, Downloaded from https://onlinelibrary.wiley.com/doi/10.1002/cbin.12161 by UNIP - Universidade Paulista, Wiley Online Library on [04/07/2025]. See the Terms and Conditions (https://onlinelibrary.wiley.com/terms-and-conditions) on Wiley Online Library for rules of use; OA articles are governed by the applicable Creative Commons License

Marumoto, A., Milani, R., da Silva, R. A., da Costa Fernandes, C. J., Granjeiro, J. M., Ferreira, C. V., Peppelenbosch, M. P., & Zambuzzi, W. F. (2017). Phosphoproteome analysis reveals a critical role for hedgehog signalling in osteoblast morphological transitions. *Bone*, *103*, 55–63. https://doi.org/10.1016/j.bone.2017.06.012

Rasmussen, K. D., & Helin, K. (2016). Role of TET enzymes in DNA methylation, development, and cancer. *Genes & Development*, *30*(7), 733–750. https://doi.org/10.1101/gad.276568.115

Rio, D. C., Ares, M., Hannon, G. J., & Nilsen, T. W. (2010). Purification of RNA using TRIzol (TRI reagent). *Cold Spring Harbor Protocols*, *2010*(6), pdb.prot5439. https://doi.org/10.1101/pdb.prot5439

da S. Feltran, G., Bezerra, F., da Costa Fernandes, C. J., Ferreira, M. R., & Zambuzzi, W. F. (2019). Differential inflammatory landscape stimulus during titanium surfaces obtained osteogenic phenotype. *Journal of Biomedical Materials Research. Part A*, *107*(8), 1597–1604. https://doi.org/10.1002/jbm.a.36673

da Silva, R. A., Fernandes, C. J. C., Feltran, G. S., Gomes, A. M., de Camargo Andrade, A. F., Andia, D. C., Peppelenbosch, M. P., & Zambuzzi, W. F. (2019). Laminar shear stress-provoked cytoskeletal changes are mediated by epigenetic reprogramming of TIMP1 in human primary smooth muscle cells. *Journal of Cellular Physiology*, *234*(5), 6382–6396. https://doi.org/10.1002/jcp.27374

da Silva, R. A., Fuhler, G. M., Janmaat, V. T., da C. Fernandes, C. J., da Silva Feltran, G., Oliveira, F. A., Matos, A. A., Oliveira, R. C., Ferreira, M. R., Zambuzzi, W. F., & Peppelenbosch, M. P. (2019). HOXA cluster gene expression during osteoblast differentiation involves epigenetic control. *Bone*, *125*, 74–86. https://doi.org/10.1016/j.bone.2019.04.026

da Silva, R. A., da S Feltran, G., da C Fernandes, C. J., & Zambuzzi, W. F. (2020). Osteogenic gene markers are epigenetically reprogrammed during contractile-to-calcifying vascular smooth muscle cell phenotype transition. *Cellular Signalling*, *66*, 109458. https://doi.org/10.1016/j.cellsig.2019.109458

da Silva Feltran, G., da Costa Fernandes, C. J., Rodrigues Ferreira, M., Kang, H. R., de Carvalho Bovolato, A. L., de Assis Golim, M., Deffune, E., Koh, I. H. J., Constantino, V. R. L., & Zambuzzi, W. F. (2019). Sonic hedgehog drives layered double hydroxides-induced acute inflammatory landscape. *Colloids and Surfaces B: Biointerfaces*, *174*, 467–475. https://doi.org/10.1016/j.colsurfb.2018.11.051

Spinella-Jaegle, S., Rawadi, G., Kawai, S., Gallea, S., Faucheu, C., Mollat, P., Courtois, B., Bergaud, B., Ramez, V., Blanchet, A. M., Adelmant, G., Baron, R., & Roman-Roman, S. (2001). Sonic hedgehog increases the commitment of pluripotent mesenchymal cells into the osteoblastic lineage and abolishes adipocytic differentiation. *Journal of Cell Science*, *114*(Pt 11), 2085–2094. https://doi.org/10.1242/jcs.114.11.2085

Tian, Y., Xu, Y., Fu, Q., & Dong, Y. (2012). Osterix is required for Sonic hedgehog-induced osteoblastic MC3T3-E1 cell differentiation. *Cell Biochemistry and Biophysics*, *64*(3), 169–176. https://doi.org/10.1007/s12013-012-9369-7

Untergasser, A., Cutcutache, I., Koressaar, T., Ye, J., Faircloth, B. C., Remm, M., & Rozen, S. G. (2012). Primer3—New capabilities and interfaces. *Nucleic Acids Research*, *40*(15), e115. https://doi.org/10.1093/nar/gks596

Vrtačnik, P., Marc, J., & Ostanek, B. (2014). Epigenetic mechanisms in bone. *Clinical Chemistry and Laboratory Medicine*, *52*(5), 589–608. https://doi.org/10.1515/cclm-2013-0770

Wang, C., Shan, S., Wang, C., Wang, J., Li, J., Hu, G., Dai, K., Li, Q., & Zhang, X. (2017). Mechanical stimulation promote the osteogenic differentiation of bone marrow stromal cells through epigenetic regulation of Sonic Hedgehog. *Experimental Cell Research*, *352*(2), 346–356. https://doi.org/10.1016/j.yexcr.2017.02.021

Yamaguchi, A., Komori, T., & Suda, T. (2000). Regulation of osteoblast differentiation mediated by bone morphogenetic proteins, hedgehogs, and Cbfa1. *Endocrine Reviews*, *21*(4), 393–411. https://doi.org/10.1210/edrv.21.4.0403

Zhou, Y., Yang, Y., Dong, R., & Huang, Y. (2023). Regulation of Shh/Bmp4 signaling pathway by DNA methylation in rectal nervous system development of fetal rats with anorectal malformation. *Journal of Pediatric Surgery*, *58*(7), 1317–1321. https://doi.org/10.1016/j.jpedsurg.2023.01.062

**How to cite this article:** Feltran, G. d. S., Andrade, A. F. d., Fernandes, C. J. d. C., Silva, R. A. F. d., & Zambuzzi, W. F. (2024). BMP7-induced osteoblast differentiation requires hedgehog signaling and involves nuclear mechanisms of gene expression control. *Cell Biology International*, *48*, 939–950. https://doi.org/10.1002/cbin.12161

10958355, 2024, 7, Downloaded from https://onlinelibrary.wiley.com/doi/10.1002/cbin.12161 by UNIP - Universidade Paulista, Wiley Online Library on [04/07/2025]. See the Terms and Conditions (https://onlinelibrary.wiley.com/terms-and-conditions) on Wiley Online Library for rules of use; OA articles are governed by the applicable Creative Commons License